



## OPEN ACCESS

## EDITED BY

Giuseppe Cardillo,  
San Camillo Forlanini Hospital, Italy

## REVIEWED BY

Bilgin Kadri Aribas,  
Bülent Ecevit University, Türkiye  
Dulio Divisi,  
University of L'Aquila, Italy

## \*CORRESPONDENCE

Xiaopeng Zhang  
✉ lzky123@163.com

<sup>†</sup>These authors have contributed equally to this work and share first authorship

RECEIVED 09 March 2023

ACCEPTED 15 May 2023

PUBLISHED 24 May 2023

## CITATION

Li Z, Zhao Q, Wu W, Hu Z and Zhang X (2023) Analysis of bronchovascular patterns in the left superior division segment to explore the relationship between the descending bronchus and the artery crossing intersegmental planes. *Front. Oncol.* 13:1183227. doi: 10.3389/fonc.2023.1183227

## COPYRIGHT

© 2023 Li, Zhao, Wu, Hu and Zhang. This is an open-access article distributed under the terms of the [Creative Commons Attribution License \(CC BY\)](https://creativecommons.org/licenses/by/4.0/). The use, distribution or reproduction in other forums is permitted, provided the original author(s) and the copyright owner(s) are credited and that the original publication in this journal is cited, in accordance with accepted academic practice. No use, distribution or reproduction is permitted which does not comply with these terms.

# Analysis of bronchovascular patterns in the left superior division segment to explore the relationship between the descending bronchus and the artery crossing intersegmental planes

Zhikai Li<sup>1,2†</sup>, Qingtao Zhao<sup>2†</sup>, Wenbo Wu<sup>2†</sup>, Zhonghui Hu<sup>2†</sup> and Xiaopeng Zhang<sup>2\*</sup>

<sup>1</sup>Graduate School, Hebei Medical University, Shijiazhuang, China, <sup>2</sup>Department of Thoracic Surgery, Hebei General Hospital, Shijiazhuang, China

**Background:** A comprehensive understanding of the anatomical variations in the pulmonary bronchi and arteries is particularly essential to the implementation of safe and precise left superior division segment (LSDS) segmentectomy. However, no report shows the relationship between the descending bronchus and the artery crossing intersegmental planes. Thus, the purpose of the present study was to analyze the branching pattern of the pulmonary artery and bronchus in LSDS using three-dimensional computed tomography bronchography and angiography (3D-CTBA) and to explore the associated pulmonary anatomical features of the artery crossing intersegmental planes.

**Materials and methods:** The 3D-CTBA images of 540 cases were retrospectively analyzed. We reviewed the anatomical variations of the LSDS bronchus and artery and assorted them according to different classifications.

**Results:** Among all 540 cases of 3D-CTBA, there were 16 cases (44.4%) with lateral subsegmental artery crossing intersegmental planes (AX<sup>3</sup>a), 20 cases (55.6%) Without AX<sup>3</sup>a in the descending B<sup>3</sup>a or B<sup>3</sup> type, and 53 cases (10.5%) with AX<sup>3</sup>a, 451 cases (89.5%) Without AX<sup>3</sup>a in the Without the descending B<sup>3</sup>a or B<sup>3</sup> type. This illustrated that the AX<sup>3</sup>a was more common in the descending B<sup>3</sup>a or B<sup>3</sup> type ( $P < 0.005$ ). Similarly, there were 69 cases (36.1%) with horizontal subsegmental artery crossing intersegmental planes (AX<sup>1+2</sup>c), 122 cases (63.9%) Without AX<sup>1+2</sup>c in the descending B<sup>1+2</sup>c type, and 33 cases (9.5%) with AX<sup>1+2</sup>c, 316 cases (90.5%) Without AX<sup>1+2</sup>c in the Without the descending B<sup>1+2</sup>c type. Combinations of the branching patterns of the AX<sup>1+2</sup>c and the descending B<sup>1+2</sup>c type were significantly dependent ( $p < 0.005$ ). The combinations of the branching patterns of the AX<sup>1+2</sup>c and the descending B<sup>1+2</sup>c type were frequently observed.

**Conclusions:** This is the first report to explore the relationship between the descending bronchus and the artery crossing intersegmental planes. In patients with the descending B<sup>3</sup>a or B<sup>3</sup> type, the incidence of the AX<sup>3</sup>a was increased. Similarly, the incidence of the AX<sup>1 + 2</sup>c was increased in patients with the descending B<sup>1 + 2</sup>c type. These findings should be carefully identified when performing an accurate LSDS segmentectomy.

#### KEYWORDS

left superior division segment (LSDS), anatomical variation, artery crossing intersegmental planes, non-small cell lung carcinoma (NSCLC), segmentectomy, video-assisted thoracoscopic surgery (VATS)

## Introduction

With the widespread use of High-resolution computed tomography (HRCT), an increasing number of ground-glass opacities (GGOs) are being identified. Several studies have shown the same oncologic efficacy between a video-assisted thoracoscopic surgery (VATS) lobectomy and segmentectomy for GGO-dominant peripheral lung cancer (1–7).

The JCOG0804 study evaluates the efficacy and safety of sublobar resection for GGO-dominant peripheral lung cancer with consolidation tumor ratio  $\leq 0.25$  and maximum tumor diameter  $\leq 2.0$  cm (1). Based on the result of JCOG0804, sublobar resection with enough surgical margin offered sufficient local control and relapse-free survival (RFS) for GGO-dominant peripheral lung cancer (1). The JCOG0802 study is a randomized, controlled, non-inferiority trial to confirm whether segmentectomy is not inferior to lobectomy regarding prognosis (2, 3). The JCOG0802 study showed segmentectomy to be non-inferior and superior to lobectomy with regards to overall survival (OS) and concluded segmentectomy should be the standard surgical procedure, rather than lobectomy, for patients with small-sized ( $\leq 2$  cm, consolidation-to-tumor ratio  $>0.5$ ) peripheral non-small cell lung carcinoma (NSCLC) (2, 3).

The primary forms of sublobar resection currently contain wedge resection and anatomical segmentectomy. However, VATS segmentectomy is more complex than a standard lobectomy because of the anatomical sophistication of the lung, characterizing both segmental vessels and bronchi structures that diversify at different levels. Therefore, comprehensive knowledge of the pulmonary bronchovascular pattern by general thoracic surgeons has become more significant to the implementation of safe and precise left superior

division segment (LSDS) surgery. However, only a few studies represent anatomic variations of the LSDS using three-dimensional computed tomography bronchography and angiography (3D-CTBA) (8–12). Moreover, we also found the aberrant artery crossing intersegmental planes in LSDS (13). The purpose of the present study was to classify the branching patterns of the left superior division bronchus (LSDB) and the left superior division artery (LSDA) by using data obtained from 3D-CTBA. Furthermore, we explore the associated anatomical features of artery crossing intersegmental planes in LSDS.

## Methods

### Patient preparation and reconstruction of 3D-CTBA

The inclusion and exclusion criteria of this study:

Inclusion criteria:

- ①. GGO, with a diameter of less than 2 cm and with a consolidation tumor ratio of less than 25%, situated in the left upper lobe (LUL);
- ②. Sublobar resection (segmentectomy or wedge resection) was implemented;
- ③. Patients underwent routine chest-enhanced CT examinations preoperatively.
- ④. Without a history of left lung surgery;

Exclusion criteria:

- ①. The images showed by enhanced CT lung examination were not distinct, which influenced the three-dimensional (3D) reconstruction of the lung;
- ②. The lesion size of the LUL exceeded 3cm.

From October 2020 to October 2022, 540 patients (248 men, 292 women; mean age, 56 years) were enrolled from the Department of Thoracic Surgery, Hebei General Hospital. After collecting CT data, the volume data from both arterial and venous

**Abbreviations:** 3D-CTBA, three-dimensional computed tomography bronchography and angiography; NSCLC, non-small cell lung carcinoma; GGOs, ground glass opacities; HRCT, high-resolution computed tomography; VATS, video-assisted thoracoscopic surgery; RFS, relapse-free survival; OS, overall survival; LMB, left main bronchus; LUL, left upper lobe; LLL, left lower lobe; LSDS, left superior division segment; LS, lingular segment; LSDB, left superior division bronchus; LSDA, left superior division artery; LSB, lingular segment bronchus; LSA, lingular segment artery; LPA, left pulmonary artery; 3D, three-dimensional.

phases were imported into a reconstruction software (Infer Operate Thorax Planning), which computed and processed the data before presenting it in 3D-CTBA images (14). All procedures involving human participants in this study were in accordance with the Declaration of Helsinki (revised in 2013). The Research Ethics Committee approved this retrospective study at Hebei General Hospital (no. 2022119). The need for patient consent was waived because of the retrospective nature of the study. Variations in the LSDA and LSDB were classified and summarized.

### Definition of each segment in the LUL

The LSDS and lingular segment (LS) form LUL. The LUL was sorted into the apicoposterior segment ( $S^{1+2}$ ), anterior segment ( $S^3$ ), superior lingular segment ( $S^4$ ), and inferior lingular segment ( $S^5$ ).  $S^{1+2}$  and  $S^3$  were subclassified into three pulmonary subsegments ( $S^{1+2a}$ ,  $S^{1+2b}$ ,  $S^{1+2c}$ ,  $S^3a$ ,  $S^3b$ ,  $S^3c$ ) respectively. The LSDS consists of  $S^{1+2}$  and  $S^3$ . The LS is comprised of  $S^4$  and  $S^5$ .

### Definition of the LSDB and lingular segment bronchus (LSB)

Segmental and subsegmental bronchi of LSDB were nominated (10):  $B^{1+2}$  is the apicoposterior segmental bronchus that divides into

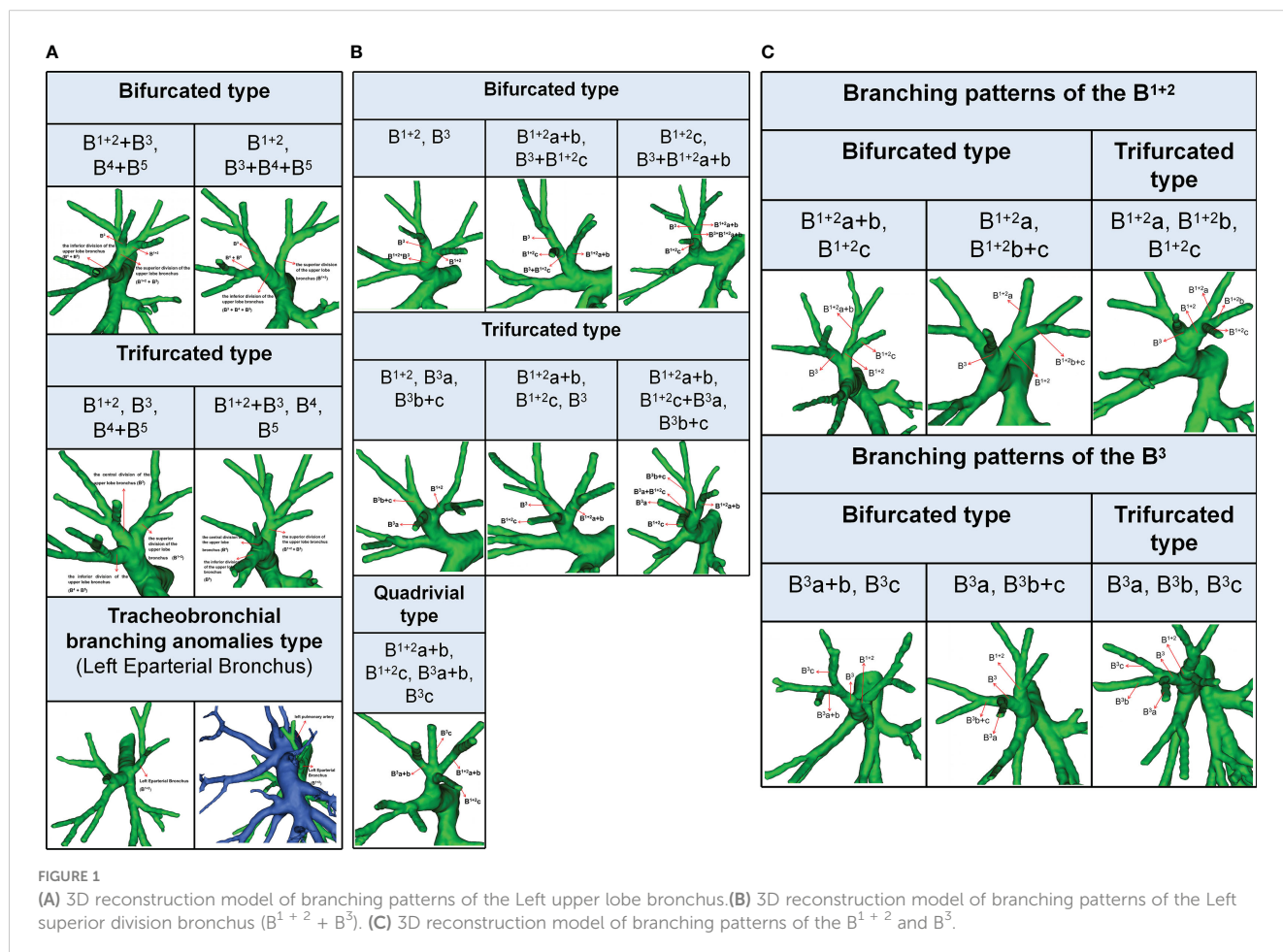
apical ( $B^{1+2a}$ ), posterior ( $B^{1+2b}$ ) and horizontal ramus ( $B^{1+2c}$ );  $B^3$  is the anterior segmental bronchus that is further sorted into lateral ( $B^3a$ ), medial ( $B^3b$ ) and superior ramus ( $B^3c$ ) (Figure 1). LSB divides into superior ( $B^4$ ) and inferior ( $B^5$ ) segmental bronchi (Figure 1).

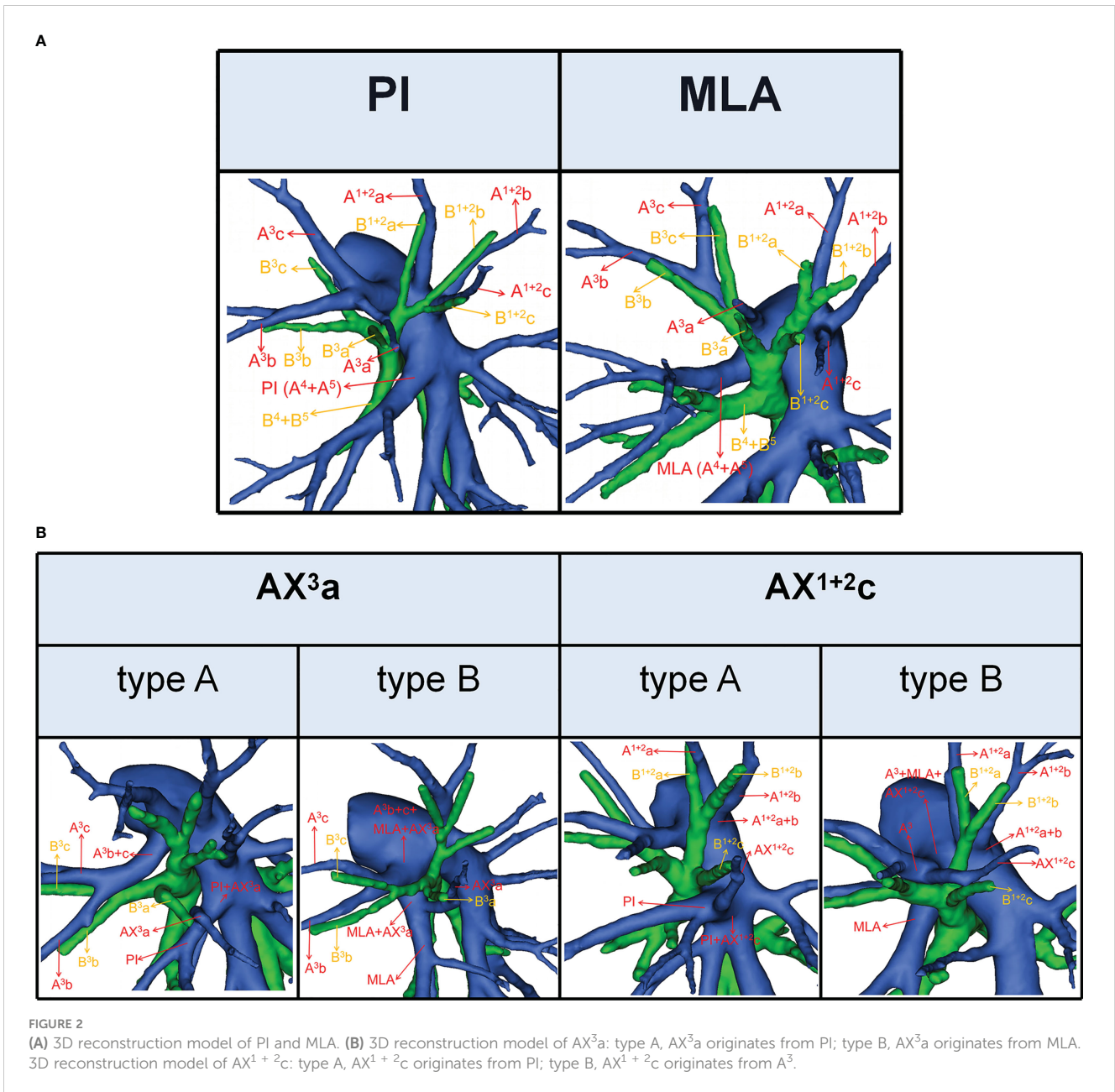
According to the classification proposed by Dominique (15), the term left eparterial bronchus refers to any bronchus directed toward the LUL that originates from the left main bronchus (LMB) above the level where the left pulmonary artery (LPA) crosses the LMB (Figure 1A).

### Definition of the LSDA and the lingular segment artery (LSA)

Segmental and subsegmental arteries of LSDA were named (10):  $A^{1+2}$  is the apicoposterior segmental artery that divides into apical ( $A^{1+2a}$ ), posterior ( $A^{1+2b}$ ) and horizontal ramus ( $A^{1+2c}$ );  $A^3$  is the anterior segmental artery that is further sorted into lateral ( $A^3a$ ), medial ( $A^3b$ ) and superior ramus ( $A^3c$ ) (Figure 2A). The LSA was comprised of the superior lingular artery ( $A^4$ ) and inferior lingular artery ( $A^5$ ).

According to the origin of LSA, the nomenclature of LSA was divided into two types (11): PI, which originates from the interlobar portion of the LPA; MLA, which originates from the mediastinal portion of the LPA (Figure 2A).





### Definition of the artery crossing intersegmental planes

The lateral subsegmental artery crossing intersegmental planes was defined as the AX<sup>3</sup>a (16). And AX<sup>3</sup>a has two origins (Figure 2B). When AX<sup>3</sup>a originates from PI, it spans the intersegmental planes between S<sup>3</sup> and S<sup>4</sup> and supplies S<sup>3</sup>a (Figure 2B). Similarly, when AX<sup>3</sup>a originates from MLA, it also spans the intersegmental planes between S<sup>3</sup> and S<sup>4</sup> and supplies S<sup>3</sup>a (Figure 2B).

The horizontal subsegmental artery crossing intersegmental planes was named as AX<sup>1+2</sup>c. Moreover, AX<sup>1+2</sup>c has two origins (Figure 2B). When AX<sup>1+2</sup>c originates from PI, it spans the intersegmental planes between S<sup>3</sup> and S<sup>4</sup> and supplies S<sup>1+2</sup>c (Figure 2B). However, when AX<sup>1+2</sup>c originates from A<sup>3</sup>, it spans the intersegmental planes between S<sup>1+2</sup> and S<sup>3</sup> and supplies S<sup>1+2</sup>c (Figure 2B).

### Statistics

All statistical analyses were implemented using SPSS 23.0 (SPSS, Chicago, IL, USA). Qualitative data were presented as the number of cases (percentage). The Pearson Chi-Square test was used to evaluate the significance of dependencies between the groups. A P-value less than 0.05 was considered statistically significant.

### Results

#### Branching patterns of the LUL bronchus

The branching patterns of the LUL bronchus were classified into three types (Table 1; Figure 1A): bifurcated type (493/540,

91.3%), trifurcated type (45/540, 8.3%), and tracheobronchial branching abnormalities type (2/540, 0.4%). The bifurcated type was further divided into two subtypes (Table 1; Figure 1A): type 1, in which a common trunk of  $B^{1+2}+B^3$  originates from the superior division of the upper lobe bronchus and a common trunk of  $B^4+B^5$  originates from the inferior division of the upper lobe bronchus (90.9%); type 2, in which  $B^{1+2}$  originates from the superior division of the upper lobe bronchus and a common trunk of  $B^3+B^4+B^5$  originates from the inferior division of the upper lobe bronchus (0.4%). The trifurcated type was also further sorted into two subtypes (Table 1; Figure 1A): type 1, in which  $B^{1+2}$  comes from the superior division of the upper lobe bronchus,  $B^3$  comes from the central division of the upper lobe bronchus, and a common trunk of  $B^4+B^5$  comes from the inferior division of the upper lobe bronchus (3.9%); type 2, in which a common trunk of  $B^{1+2}+B^3$  comes from the superior division of the upper lobe bronchus,  $B^4$  comes from the central division of the upper lobe bronchus, and  $B^5$  comes from the inferior division of the upper lobe bronchus (4.4%). Moreover,  $B^{1+2}$  originating from the LMB was found in 2 cases in the Left Eparterial Bronchus. The LPA was on the ventral side of  $B^{1+2}$  and did not cross the dorsal side of the LMB (Figure 1A).

### Branching patterns of the LSDB ( $B^{1+2} + B^3$ )

The branching patterns of LSDB were divided into three types (Table 2; Figure 1B): bifurcated type (305/491, 62.1%), trifurcated type (185/491, 37.7%), and quadrivial type (1/491, 0.2%). The bifurcated type was further separated into three subtypes (Table 2; Figure 1B): subtype I ( $B^{1+2}$ ,  $B^3$ ), subtype II ( $B^{1+2}a+b$ ,  $B^3+B^{1+2}c$ ), subtype III ( $B^{1+2}c$ ,  $B^3+B^{1+2}a+b$ ). These subtypes accounted for 58.7%, 2.0%, and 1.4%, respectively. The trifurcated type was also further subclassified into three subtypes: subtype I ( $B^{1+2}$ ,  $B^3a$ ,  $B^3b+c$ ) was observed in 2.2% of cases, subtype II ( $B^{1+2}a+b$ ,  $B^{1+2}c$ ,  $B^3$ ) was the most common (35.0%) and subtype III ( $B^{1+2}a+b$ ,  $B^{1+2}c+B^3a$ ,  $B^3b+c$ ) was seen in 2 cases (0.4%). The quadrivial type ( $B^{1+2}a+b$ ,  $B^{1+2}c$ ,  $B^3a$ ,  $B^3c$ ) was the less common (0.2%).

### Branching patterns of the $B^{1+2}$ , $B^3$

The branching pattern of  $B^{1+2}$  included two types: 522 cases were bifurcated, while trifurcated was found only in 18 cases (Table 3; Figure 1C). The bifurcated type was further divided into subtype I ( $B^{1+2}a+b$ ,  $B^{1+2}c$ ), which was presented in 488 patients (90.4%) and subtype II ( $B^{1+2}a$ ,  $B^{1+2}b+c$ ), that was occurred in 34 patients (6.3%) (Figure 1C). Similarly, the branching pattern of  $B^3$  contained two types: bifurcated type (445/540, 82.4%) and trifurcated type (95/540, 17.6%) (Table 3; Figure 1C). The bifurcated type was further divided into subtype I ( $B^3a+b$ ,  $B^3c$ ), which was found in 70 patients (13.0%) and subtype II ( $B^3a$ ,  $B^3b+c$ ), which was the most common (69.4%) (Figure 1C).

### Branching patterns of the $A^3$

According to the original location and the number of the  $A^3$ , the branching patterns of the  $A^3$  were classified and summarized in detail (Table 4; Figure 3). When the composition of the  $A^3$  included a single branch, the branching patterns of the  $A^3$  were classified into two types: type A,  $A^3$  from the anterior portion of LPA (83.0%); type B,  $A^3$  from the interlobar portion of LPA (0.5%). When the composition of the  $A^3$  contained two branches, the branching patterns of the  $A^3$  were divided into four types: type A,  $A^3b+c$  from the anterior portion of LPA and  $AX^3a$  from MLA (4.6%); type B,  $A^3b+c$  from the anterior portion of LPA and  $AX^3a$  from PI (8.1%); type C,  $A^3b+c$  from the anterior portion of LPA and  $A^3a$  from the interlobar portion of LPA (Independent  $A^3a$ ) (3.0%); type D,  $A^3b+c$  from the anterior portion of LPA and  $A^3a$  from the interlobar portion of LPA ( $A^3a$  and  $A^{1+2}c$  share a common trunk) (0.7%). As detailed in Table 4, the incidence of  $AX^3a$  was 12.8% (69/540). Furthermore, we summarized the distribution of  $AX^3a$  in bronchus type (Table 5).

### Combinations of branching patterns of $AX^3a$ and the descending $B^3a$ or $B^3$ type

In the following types (Table 2; Figure 1B),  $B^{1+2}$ ,  $B^3a$ ,  $B^3b+c$  (2.2%) and  $B^{1+2}a+b$ ,  $B^{1+2}c+B^3a$ ,  $B^3b+c$  (0.4%), the components of

TABLE 1 Branching patterns of the Left upper lobe bronchus.

	Our study (n=540)		Maki (n=539)		Deng (n=103)		Wang (n=166)	
	NO.	%	NO.	%	NO.	%	NO.	%
Bifurcated type	493	91.3	528	98.0	92	89.3	165	99.4
$B^{1+2}+B^3$ , $B^4+B^5$	491	90.9	528	98.0	92	89.3	164	98.8
$B^{1+2}$ , $B^3+B^4+B^5$	2	0.4	NR	-	NR	-	1	0.6
Trifurcated type	45	8.3	9	1.7	11	10.7	1	0.6
$B^{1+2}$ , $B^3$ , $B^4+B^5$	21	3.9	9	1.7	11	10.7	1	0.6
$B^{1+2}+B^3$ , $B^4$ , $B^5$	24	4.4	NR	-	NR	-	NR	-
Tracheobronchial branching anomalies type	2	0.4	2	0.3	NR	-	NR	-
Left Eparterial Bronchus	2	0.4	2	0.3	NR	-	NR	-

NR: the type was not referred

TABLE 2 Branching patterns of the Left superior division bronchus ( $B^{1+2} + B^3$ ).

	Our study (n=491)		Maki (n=537)		Deng (n=92)		Wang (n=166)	
	NO.	%	NO.	%	NO.	%	NO.	%
Bifurcated type	305	62.1	408	76.0	92	100.0	109	65.7
$B^{1+2}, B^3$	288	58.7	408	76.0	92	100.0	102	61.4
$B^{1+2}a+b, B^3+B^{1+2}c$	10	2.0	NR	-	NR	-	6	3.6
$B^{1+2}c, B^3+B^{1+2}a+b$	7	1.4	NR	-	NR	-	NR	-
$B^{1+2}+B^3c, B^3a+b$	NR	-	NR	-	NR	-	1	0.6
Trifurcated type	185	37.7	129	24.0	NR	-	57	34.3
$B^{1+2}, B^3a, B^3b+c$	11	2.2	18	3.4	NR	-	8	4.8
$B^{1+2}a+b, B^{1+2}c, B^3$	172	35.0	109	20.3	NR	-	48	28.9
$B^{1+2}a+b, B^{1+2}c+B^3a, B^3b+c$	2	0.4	NR	-	NR	-	NR	-
$B^{1+2}a, B^{1+2}b+c, B^3$	NR	-	NR	-	NR	-	1	0.6
$B^{1+2}, B^3a+b, B^3c$	NR	-	2	0.3	NR	-	NR	-
Quadrivial type	1	0.2	NR	-	NR	-	NR	-
$B^{1+2}a+b, B^{1+2}c, B^3a+b, B^3c$	1	0.2	NR	-	NR	-	NR	-

NR: the type was not referred

$B^3$  comprised the descending  $B^3a$ . Similarly, in the following types (Table 1; Figure 1A),  $B^{1+2}, B^3, B^4+B^5$  (3.9%) and  $B^{1+2}, B^3+B^4+B^5$  (0.4%), the components of  $B^3$  comprised the descending  $B^3$ . As shown in Figure 4 and Table 6, the incidence of  $AX^3a$  with and without the descending  $B^3a$  or  $B^3$  type was 44.4% (16/36) and 10.5% (53/504), respectively. This indicated that the  $AX^3a$  was more common in the descending  $B^3a$  or  $B^3$  type ( $P < 0.005$ ).

### Branching patterns of the $A^{1+2}$

According to the original location and the number of the  $A^{1+2}$ , the branching patterns of the  $A^{1+2}$  were also sorted and summarized in detail (Table 7; Figure 5). When the composition of the  $A^{1+2}$  consisted of a single branch (Figure 5A), two types were defined: type A,  $A^{1+2}$  from the posterolateral portion of LPA

TABLE 3 Branching patterns of the  $B^{1+2}$  and Branching patterns of the  $B^3$ .

	Our study (n=540)		Wang (n=166)	
	NO.	%	NO.	%
<b>Branching patterns of the <math>B^{1+2}</math></b>				
Bifurcated type	522	96.7	166	100.0
$B^{1+2}a+b, B^{1+2}c$	488	90.4	156	94.0
$B^{1+2}a, B^{1+2}b+c$	34	6.3	10	6.0
Trifurcated type	18	3.3	NR	-
$B^{1+2}a, B^{1+2}b, B^{1+2}c$	18	3.3	NR	-
<b>Branching patterns of the <math>B^3</math></b>				
Bifurcated type	445	82.4	157	94.6
$B^3a+b, B^3c$	70	13.0	19	11.4
$B^3a, B^3b+c$	375	69.4	138	83.1
Trifurcated type	95	17.6	9	5.4
$B^3a, B^3b, B^3c$	95	17.6	9	5.4

NR: the type was not referred

TABLE 4 Branching patterns of the A<sup>3</sup>.

	Our study (n=540)	
	NO.	%
one branch	451	83.5
Type A (A <sup>3</sup> from anterior portion of LPA)	448	83.0
Type B (A <sup>3</sup> from interlobar portion of LPA)	3	0.5
two branches	89	16.5
Type A (A <sup>3</sup> b+c from anterior portion of LPA and AX <sup>3</sup> a from MLA)	25	4.6
Type B (A <sup>3</sup> b+c from anterior portion of LPA and AX <sup>3</sup> a from PI)	44	8.1
Type C (A <sup>3</sup> b+c from anterior portion of LPA and A <sup>3</sup> a from interlobar portion of LPA) (Independent A <sup>3</sup> a)	16	3.0
Type D (A <sup>3</sup> b+c from anterior portion of LPA and A <sup>3</sup> a from interlobar portion of LPA) (A <sup>3</sup> a and A <sup>1+2</sup> c share a common trunk)	4	0.7

(7.4%); type B, A<sup>1+2</sup> from A<sup>3</sup> (0.7%). When the composition of the A<sup>1+2</sup> involves two branches, patients can be divided into one of the following eight types (Figure 5A): type A, A<sup>1+2</sup>a from A<sup>3</sup> and A<sup>1+2</sup>b+c from posterolateral portion of LPA (13.9%); type B, A<sup>1+2</sup>a+b from A<sup>3</sup> and A<sup>1+2</sup>c from interlobar portion of LPA (12.4%); type C, A<sup>1+2</sup>a+b from A<sup>3</sup> and A<sup>1+2</sup>c from interlobar portion of LPA (A<sup>3</sup>a and A<sup>1+2</sup>c share a common trunk) (0.7%); type D, A<sup>1+2</sup>a+b from posterolateral portion of LPA and AX<sup>1+2</sup>c from A<sup>3</sup> (2.4%); type E, A<sup>1+2</sup>a+b from posterolateral portion of LPA and AX<sup>1+2</sup>c from PI (2.4%); type F, A<sup>1+2</sup>a+b from A<sup>3</sup> and AX<sup>1+2</sup>c from PI (1.7%); type G, A<sup>1+2</sup>a from posterolateral portion of LPA and A<sup>1+2</sup>b+c from posterolateral portion of LPA (3.0%); type H, A<sup>1+2</sup>a+b from posterolateral portion of LPA and A<sup>1+2</sup>c from interlobar portion of LPA (16.5%). When the composition of the A<sup>1+2</sup> contained three branches, there are five types (Figure 5B): type A, A<sup>1+2</sup>a from A<sup>3</sup>, A<sup>1+2</sup>b from posterolateral portion of LPA and A<sup>1+2</sup>c from interlobar portion of LPA (22.4%); type B, A<sup>1+2</sup>a from A<sup>3</sup>, A<sup>1+2</sup>b from posterolateral portion of LPA and AX<sup>1+2</sup>c from PI (7.4%); type C, A<sup>1+2</sup>a from A<sup>3</sup>, A<sup>1+2</sup>b from posterolateral portion of LPA and AX<sup>1+2</sup>c from A<sup>3</sup> (2.8%); type D, A<sup>1+2</sup>a from posterolateral portion of LPA, A<sup>1+2</sup>b from posterolateral portion of LPA and AX<sup>1+2</sup>c from PI (2.2%); type E, A<sup>1+2</sup>a from posterolateral portion of LPA, A<sup>1+2</sup>b from posterolateral portion of LPA and A<sup>1+2</sup>c from interlobar portion of LPA (4.1%). As shown in Table 7, the incidence of AX<sup>1+2</sup>c was 18.9% (102/540). Furthermore, we summarized the distribution of AX<sup>1+2</sup>c in bronchus type (Table 8).

### Combinations of branching patterns of AX<sup>1+2</sup>c and the descending B<sup>1+2</sup>c type

In the following types (Table 2; Figure 1B), B<sup>1+2</sup>a+b, B<sup>3</sup>+B<sup>1+2</sup>c (2.0%), B<sup>1+2</sup>c, B<sup>3</sup>+B<sup>1+2</sup>a+b (1.4%), B<sup>1+2</sup>a+b, B<sup>1+2</sup>c, B<sup>3</sup> (35.0%), and B<sup>1+2</sup>a+b, B<sup>1+2</sup>c+B<sup>3</sup>a, B<sup>3</sup>b+c (0.4%), the components of B<sup>1+2</sup>

included the descending B<sup>1+2</sup>c. As shown in Figure 6 and Table 9, the incidence of AX<sup>1+2</sup>c with and without the descending B<sup>1+2</sup>c type was 36.1% (69/191) and 9.5% (33/349), respectively. Combinations of the branching patterns of the AX<sup>1+2</sup>c and the descending B<sup>1+2</sup>c type were significantly dependent ( $p < 0.005$ ). This indicates that the incidence of AX<sup>1+2</sup>c was increased in patients with the descending B<sup>1+2</sup>c type.

## Discussion

The low-dose thin-slice chest CT has extremely boosted the screening rate of GGOs. Some previous studies indicated that sublobar resection should be the standard surgical procedure for patients with GGO-dominant peripheral NSCLC (1–7). Identification and dissection of the branch of LSDA are significant parts of the LSDS anatomic segmentectomy. The anatomical variations of the branching pattern in the LSDA are diverse, which extraordinarily augments the challenge in the VATS segmentectomy of the LSDS. Intraoperative misunderstandings of the branch of LSDA can result in serious complications, such as uncontrollable intraoperative bleeding that convert to open thoracotomy. Moreover, pulmonary arterial injury, particularly the LUL, was a common source of hemorrhage (17). Therefore, thoracic surgeons must have a systemic and precise understanding of the branching pattern in the LSDA.

Fortunately, advances in HRCT and reconstruction techniques have allowed for the visualization of the branching pattern of the bronchus and vascular of the lungs (18, 19). The efficacy of blood vessel visualization is reportedly about 95.2% (20). The literature illustrated that 3D-CTBA is a valuable tool for thoracic surgeons to implement segmentectomy or subsegmentectomy procedures, which decreases operative-related complications and operation time and guarantees safe surgical margins (19).



TABLE 5 Distribution of the AX<sup>3</sup>a in bronchus type.

	With AX <sup>3</sup> a	Without AX <sup>3</sup> a	total
Bronchus type			
B <sup>1+2</sup> +B <sup>3</sup> , B <sup>4</sup> +B <sup>5</sup>			
B <sup>1+2</sup> , B <sup>3</sup>	48	240	288
B <sup>1+2</sup> a+b, B <sup>3</sup> +B <sup>1+2</sup> c	0	10	10
B <sup>1+2</sup> c, B <sup>3</sup> +B <sup>1+2</sup> a+b	0	7	7
B <sup>1+2</sup> , B <sup>3</sup> a, B <sup>3</sup> b+c	7	4	11
B <sup>1+2</sup> a+b, B <sup>1+2</sup> c, B <sup>3</sup>	5	167	172
B <sup>1+2</sup> a+b, B <sup>1+2</sup> c+B <sup>3</sup> a, B <sup>3</sup> b+c	1	1	2
B <sup>1+2</sup> a+b, B <sup>1+2</sup> c, B <sup>3</sup> a, B <sup>3</sup> b+c	0	1	1
B <sup>1+2</sup> , B <sup>3</sup> +B <sup>4</sup> +B <sup>5</sup>	0	2	2
B <sup>1+2</sup> , B <sup>3</sup> , B <sup>4</sup> +B <sup>5</sup>	8	13	21
B <sup>1+2</sup> +B <sup>3</sup> , B <sup>4</sup> , B <sup>5</sup>	0	24	24
Left Eparterial Bronchus	0	2	2
total	69	471	540

are identified, it is crucial to keep an eye on the existence of the Left Eparterial Bronchus.

We found that the branching patterns of the LSDB had three types (Table 2; Figure 1B): bifurcated type (62.1%), which incidence was lower than that of Maki (76.0%) and Wang (65.7%); trifurcated type (37.7%), which was considerably higher than the frequency reported by Maki (24.0%) and Wang (34.3%); quadrivial type (0.2%), which was not found by Maki and Wang (8–10). In the bifurcated type, the B<sup>1+2</sup>, B<sup>3</sup> type was the most common type (58.7%) and the B<sup>1+2</sup>c, B<sup>3</sup>+B<sup>1+2</sup>a+b type was first reported (8–10). However, we have not found the B<sup>1+2</sup>+B<sup>3</sup>c, B<sup>3</sup>a+b type (10). For the B<sup>1+2</sup>a+b, B<sup>3</sup>+B<sup>1+2</sup>c type, a mistaken ligation of the trunk of B<sup>3</sup>+B<sup>1+2</sup>c will result in lung volume loss in the S<sup>3</sup> segmentectomy (Figure 1B). In trifurcated type, the B<sup>1+2</sup>a+b, B<sup>1+2</sup>c, B<sup>3</sup> type was the most common type (35.0%), and the B<sup>1+2</sup>a+b, B<sup>1+2</sup>c+B<sup>3</sup>a, B<sup>3</sup>b+c type was not found in the previous literature. For the B<sup>1+2</sup>a+b, B<sup>1+2</sup>c+B<sup>3</sup>a, B<sup>3</sup>b+c type, a mistaken ligation of the trunk of B<sup>1+2</sup>c+B<sup>3</sup>a will lead to the enlarged intersegmental plane in the S<sup>1+2</sup>c segmentectomy (Figure 1B). Moreover, the B<sup>1+2</sup>a, B<sup>1+2</sup>b+c, B<sup>3</sup> type and B<sup>1+2</sup>, B<sup>3</sup>a+b, B<sup>3</sup>c type were not detected in our study (8, 10).

We also observed that the branching patterns of the B<sup>1+2</sup> had two types (Table 3; Figure 1C): the bifurcated type(96.7%), which incidence was similar to that of Wang (100.0%), and the trifurcated type (3.3%), which has not been reported in the literature (10). Moreover, the classification of the branching patterns of the B<sup>3</sup> was the same as that of Wang (Table 3).

To our knowledge, the detailed classification of branching patterns of the A<sup>3</sup> was first reported (Table 4; Figure 3). An understanding of the origin of the A<sup>3</sup> branch is essential in clinical practice if a safe and precise S<sup>3</sup> segmentectomy is to be

implemented. When A<sup>3</sup> originates from the interlobar portion of LPA, A<sup>3</sup> can usually be identified by dissecting interlobar fissures. When AX<sup>3</sup>a arose from PI, AX<sup>3</sup>a should be carefully dissected from PI before it is ligated to avoid injuring PI. When a common trunk of A<sup>1+2</sup>c and A<sup>3</sup>a directly originated from the interlobar portion of the LPA, A<sup>3</sup>a should be resected without resecting A<sup>1+2</sup>c.

In the case of S<sup>3</sup>a segmentectomy, it is necessary to investigate the origin of A<sup>3</sup>a. In the present study, A<sup>3</sup>a arose from the interlobar portion of LPA in 20 cases (3.7%) (Table 4; Figure 3). This compares with the figures showed by Maki (3.9%) and Murota (8.4%) (8, 11). AX<sup>3</sup>a originating from the PI was observed in cases (8.1%), which incidence was similar to that of Maki (6.1%) and Murota (8.1%) (8, 11). Moreover, AX<sup>3</sup>a originating from MLA occurred in 25 patients (4.6%) and was the first reported (Figure 2B).

In our study, an interesting finding concerned the AX<sup>3</sup>a (Table 5; Figure 4). There was a significant correlation between the branching patterns of the AX<sup>3</sup>a and the descending B<sup>3</sup>a or B<sup>3</sup> type (Table 6). Moreover, the incidence of AX<sup>3</sup>a was increased in patients with the descending B<sup>3</sup>a or B<sup>3</sup> type (P < 0.005). This can be clarified by the paralleling correlation between pulmonary segmental arteries and pulmonary segmental bronchi. Thus, when the AX<sup>3</sup>a is identified preoperatively, the thoracic surgeons must investigate the possibility of the descending B<sup>3</sup>a or B<sup>3</sup>. For B<sup>1+2</sup>, B<sup>3</sup>a, B<sup>3</sup>b+c type, when S<sup>3</sup>a segmentectomy was planned and performed, it was practical and safe to ligate the AX<sup>3</sup>a originating from PI in the side of the oblique fissure, followed by the B<sup>3</sup>a (Figure 4). For B<sup>1+2</sup>a+b, B<sup>1+2</sup>c+B<sup>3</sup>a, B<sup>3</sup>b+c type, it was easier to dissect the B<sup>3</sup>a from the oblique fissure in the S<sup>3</sup>a segmentectomy (Figure 4). And AX<sup>3</sup>a originating MLA was identified after resection B<sup>3</sup>a. At the same time, it may be disturbed by the LUL vein.

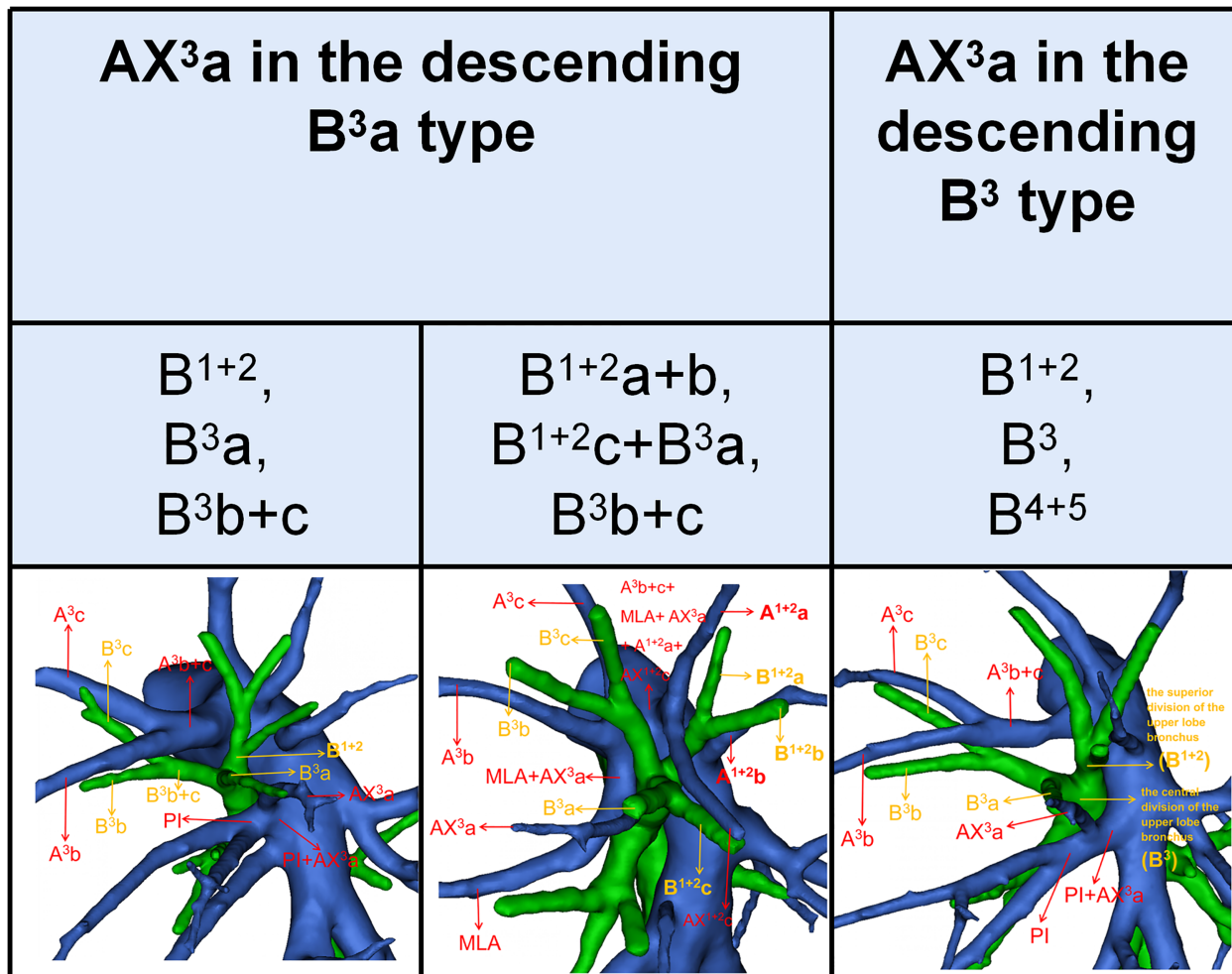


FIGURE 4 Distribution of the AX<sup>3</sup>a in the descending B<sup>3</sup>a or B<sup>3</sup> type.

It is significant to understand the branching patterns of A<sup>1+2</sup> pre-operatively (Figure 5; Table 7). When A<sup>1+2</sup> originated from the posterolateral portion of LPA (Figure 5A), during S<sup>1+2</sup>a segmentectomy, it is necessary to dissect the branches of A<sup>1+2</sup> in a center-to-periphery direction to distinguish A<sup>1+2</sup>a, A<sup>1+2</sup>b, and A<sup>1+2</sup>c. However, it significantly increased the difficulty of dissection. When A<sup>1+2</sup>a+b originated from the posterolateral portion of LPA and A<sup>1+2</sup>c originated from the interlobar portion of LPA (type H), during S<sup>1+2</sup> segmentectomy, we need

to dissect the posterolateral portion and the interlobar portion of LPA to discriminate A<sup>1+2</sup>a+b and A<sup>1+2</sup>c (Figure 5A).

As shown in Figure 5 and Table 7, the branching patterns of the A<sup>1+2</sup> in this study were somewhat different from the previous report (12). The main reason is the introduction of AX<sup>1+2</sup>c. In the present study, AX<sup>1+2</sup>c arose from the PI in 74 cases (13.7%) (Figure 2B). This compares with the figures revealed by Deng (6.8%) and Murota (3.8%) (9, 11). Moreover, AX<sup>1+2</sup>c originating from A<sup>3</sup> was observed in 28 patients (5.2%) and was the first reported (Figure 2B).

TABLE 6 Distribution of the AX<sup>3</sup>a in the descending B<sup>3</sup>a or B<sup>3</sup> type.

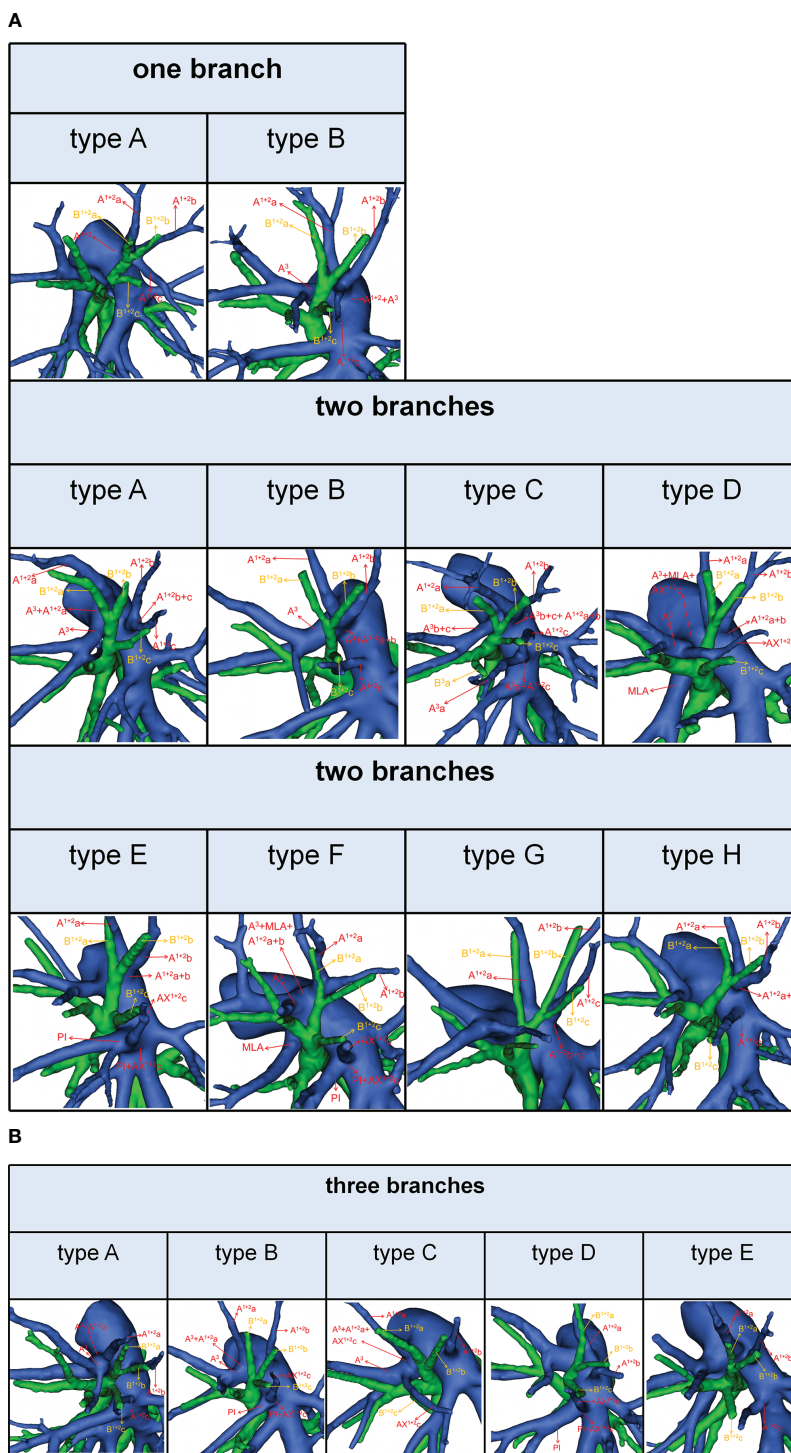
	With AX <sup>3</sup> a	Without AX <sup>3</sup> a	total	P value
With the descending B <sup>3</sup> a or B <sup>3</sup>	16	20	36	p < 0.005
Without the descending B <sup>3</sup> a or B <sup>3</sup>	53	451	504	
total	69	471	540	

TABLE 7 Branching patterns of the  $A^{1+2}$ .

	Our study(n=540)		Chen (n=404)	
	NO.	%	NO.	%
one branch	44	8.1	53	13.1
Type A ( $A^{1+2}$ from the posterolateral portion of LPA)	40	7.4	53	13.1
Type B ( $A^{1+2}$ from $A^3$ )	4	0.7	NR	-
two branches	286	53.0	254	62.9
Type A ( $A^{1+2a}$ from $A^3$ and $A^{1+2b+c}$ from posterolateral portion of LPA)	75	13.9	68	16.8
Type B ( $A^{1+2a+b}$ from $A^3$ and $A^{1+2c}$ from interlobar portion of LPA)	67	12.4	49	12.1
Type C ( $A^{1+2a+b}$ from $A^3$ and $A^{1+2c}$ from interlobar portion of LPA) ( $A^3a$ and $A^{1+2c}$ share a common trunk)	4	0.7	NR	-
Type D ( $A^{1+2a+b}$ from posterolateral portion of LPA and $AX^{1+2c}$ from $A^3$ )	13	2.4	NR	-
Type E ( $A^{1+2a+b}$ from posterolateral portion of LPA and $AX^{1+2c}$ from PI)	13	2.4	NR	-
Type F ( $A^{1+2a+b}$ from $A^3$ and $AX^{1+2c}$ from PI)	9	1.7	NR	-
Type G ( $A^{1+2a}$ from posterolateral portion of LPA and $A^{1+2b+c}$ from posterolateral portion of LPA)	16	3.0	28	6.9
Type H ( $A^{1+2a+b}$ from posterolateral portion of LPA and $A^{1+2c}$ from interlobar portion of LPA)	89	16.5	109	27.0
three branches	210	38.9	97	24.0
Type A ( $A^{1+2a}$ from $A^3$ , $A^{1+2b}$ from posterolateral portion of LPA, and $A^{1+2c}$ from interlobar portion of LPA)	121	22.4	66	16.3
Type B ( $A^{1+2a}$ from $A^3$ , $A^{1+2b}$ from posterolateral portion of LPA, and $AX^{1+2c}$ from PI)	40	7.4	NR	-
Type C ( $A^{1+2a}$ from $A^3$ , $A^{1+2b}$ from posterolateral portion of LPA, and $AX^{1+2c}$ from $A^3$ )	15	2.8	NR	-
Type D ( $A^{1+2a}$ from posterolateral portion of LPA, $A^{1+2b}$ from posterolateral portion of LPA, and $AX^{1+2c}$ from PI)	12	2.2	NR	-
Type E ( $A^{1+2a}$ from posterolateral portion of LPA, $A^{1+2b}$ from posterolateral portion of LPA, and $A^{1+2c}$ from interlobar portion of LPA)	22	4.1	31	7.7

$AX^{1+2c}$  is not uncommon in clinical practice; however, if it occurs, it can lead to significant difficulties for patients to perform  $S^{1+2c}$  segmentectomy. No previous report has reported the distribution of  $AX^{1+2c}$  branching patterns in the bronchus type (Table 8). Moreover, the combination of branching patterns of the  $AX^{1+2c}$  and the descending  $B^{1+2c}$  type showed significant dependence (Table 9). And it was first reported. This denoted that

the  $AX^{1+2c}$  was often combined with the descending  $B^{1+2c}$  type. The paralleling relationship between pulmonary segmental arteries and pulmonary segmental bronchi may explain this phenomenon. Thus, when the  $AX^{1+2c}$  was recognized preoperatively, it is crucial to keep an eye on the existence of the descending  $B^{1+2c}$  type. For  $B^{1+2a+b}$ ,  $B^{1+2c}$ ,  $B^3$  type, when  $S^{1+2c}$  segmentectomy was implemented, it was feasible and secured to dissect the  $AX^{1+2c}$



**FIGURE 5**  
**(A)** 3D reconstruction model of branching patterns of the  $A^{1+2}$ , when the composition of the  $A^{1+2}$  contained single branch and two branches. **(B)** 3D reconstruction model of branching patterns of the  $A^{1+2}$ , when the composition of the  $A^{1+2}$  contained three branches.

originating from PI in the side of the oblique fissure, followed by the  $B^{1+2c}$  (Figure 6). When  $AX^{1+2c}$  arose from  $A^3$ , it ran deep within the lung parenchyma of  $S^3$ . For  $B^{1+2a+b}$ ,  $B^3+B^{1+2c}$  type, it was easier to identify the  $B^{1+2c}$  from the oblique fissure in the  $S^{1+2c}$  segmentectomy (Figure 6). However, the  $AX^{1+2c}$  was exposed by

lifting the  $B^{1+2c}$  stump. And it was essential to avoid causing damage to the  $A^3$  when the  $AX^{1+2c}$  was ligated. In sum, we defined the coexistence of the  $AX^{1+2c}$  and the descending  $B^{1+2c}$ , the  $AX^3a$  and the descending  $B^3a$ , and the  $AX^3a$  and the descending  $B^3$  as “Hebei’s triad combinations”.



## Conclusions

This is the first report to explore the associated pulmonary anatomical features of AX<sup>1+2c</sup> and AX<sup>3a</sup>. We found that the incidence of AX<sup>1+2c</sup> was increased in patients with the descending B<sup>1+2c</sup> type, and AX<sup>3a</sup> was increased in patients with the descending B<sup>3a</sup> or B<sup>3</sup> type. This knowledge will assist in the preoperative planning of S<sup>1+2c</sup> segmentectomy and S<sup>3a</sup> segmentectomy.

## Data availability statement

The original contributions presented in the study are included in the article/supplementary material. Further inquiries can be directed to the corresponding author.

## Ethics statement

The Research Ethics Committee approved this retrospective study at Hebei General Hospital (no. 2022119). The need for patient consent was waived because of the retrospective nature of the study.

## Author contributions

ZL: project design and initiation, data analysis, manuscript writing. QZ: project design and initiation, data analysis, manuscript writing. WW: project design and initiation, data analysis, manuscript writing. ZH: data collection. XZ: supervisor.

## References

- Suzuki K, Watanabe SI, Wakabayashi M, Saji H, Aokage K, Moriya Y, et al. A single-arm study of sublobar resection for ground-glass opacity dominant peripheral lung cancer. *J Thorac Cardiovasc Surg* (2022) 163(1):289–301 e2. doi: 10.1016/j.jtcvs.2020.09.146
- Suzuki K, Saji H, Aokage K, Watanabe SI, Okada M, Mizusawa J, et al. Comparison of pulmonary segmentectomy and lobectomy: safety results of a randomized trial. *J Thorac Cardiovasc Surg* (2019) 158(3):895–907. doi: 10.1016/j.jtcvs.2019.03.090
- Saji H, Okada M, Tsuboi M, Nakajima R, Suzuki K, Aokage K, et al. Segmentectomy versus lobectomy in small-sized peripheral non-small-cell lung cancer (JCOG0802/WJOG4607L): a multicentre, open-label, phase 3, randomised, controlled, non-inferiority trial. *Lancet* (2022) 399(10335):1607–17. doi: 10.1016/S0140-6736(21)02333-3
- Nomori H, Shiraishi A, Cong Y, Sugimura H, Mishima S. Differences in postoperative changes in pulmonary functions following segmentectomy compared with lobectomy. *Eur J Cardiothorac Surg* (2018) 53(3):640–7. doi: 10.1093/ejcts/ezx357
- Nakamura H, Taniguchi Y, Miwa K, Adachi Y, Fujioka S, Haruki T, et al. Comparison of the surgical outcomes of thoracoscopic lobectomy, segmentectomy, and wedge resection for clinical stage I non-small cell lung cancer. *Thorac Cardiovasc Surg* (2011) 59(3):137–41. doi: 10.1055/s-0030-1250377
- Moon MH, Moon YK, Moon SW. Segmentectomy versus lobectomy in early non-small cell lung cancer of 2 cm or less in size: a population-based study. *Respirology* (2018) 23(7):695–703. doi: 10.1111/resp.13277
- Landreneau RJ, Normolle DP, Christie NA, Awais O, Wizorek JJ, Abbas G, et al. Recurrence and survival outcomes after anatomic segmentectomy versus lobectomy for clinical stage I non-small-cell lung cancer: a propensity-matched analysis. *J Clin Oncol* (2014) 32(23):2449–55. doi: 10.1200/JCO.2013.50.8762
- Maki R, Miyajima M, Ogura K, Tada M, Takahashi Y, Adachi H, et al. Pulmonary vessels and bronchus anatomy of the left upper lobe. *Surg Today* (2022) 52(4):550–8. doi: 10.1007/s00595-022-02471-1
- Deng Y, Cai S, Huang C, Liu W, Du L, Wang C, et al. Anatomical variation analysis of left upper pulmonary blood vessels and bronchi based on three-dimensional reconstruction of chest CT. *Front Oncol* (2022) 12:1028467. doi: 10.3389/fonc.2022.1028467
- He H, Wang F, Wang PY, Chen P, Li WWL, Perroni G, et al. Anatomical analysis of variations in the bronchus pattern of the left upper lobe using three-dimensional computed tomography angiography and bronchography. *Ann Transl Med* (2022) 10(6):305. doi: 10.21037/atm-22-598
- Murota M, Yamamoto Y, Satoh K, Ishimura M, Yokota N, Norikane T, et al. An analysis of anatomical variations of the left pulmonary artery of the interlobar portion for lung resection by three-dimensional CT pulmonary angiography and thin-section images. *Jpn J Radiol* (2020) 38(12):1158–68. doi: 10.1007/s11604-020-01024-1
- Gao C, Xu WZ, Li ZH, Chen L. Analysis of bronchial and vascular patterns in left upper lobes to explore the genesis of mediastinal lingular artery and its influence on pulmonary anatomical variation. *J Cardiothorac Surg* (2021) 16(1):306. doi: 10.1186/s13019-021-01682-w
- Zhang C, Li J, Sun H, Liu H. An aberrant anterior ascending segmental pulmonary artery (A3a1) in a patient with lung cancer. *Eur J Cardiothorac Surg* (2022) 61(5):1201–3. doi: 10.1093/ejcts/ezab564
- Li Z, Kong Y, Wu W, Chen S, Zhang X. What is the correlation between the defective and splitting posterior segmental bronchus and recurrent artery crossing intersegmental planes in the right upper lobe? *Front Surg* (2023) 10:1113783. doi: 10.3389/fsurg.2023.1113783
- Chassagnon G, Morel B, Carpentier E, Le Pointe HD, Sirinelli D. Tracheobronchial branching abnormalities: lobe-based classification scheme. *Radiographics* (2016) 36(2):358–73. doi: 10.1148/rg.2016150115
- Boyden EA, Hartmann JF. An analysis of variations in the bronchopulmonary segments of the left upper lobes of fifty lungs. *Am J Anat* (1946) 79(3):321–60. doi: 10.1002/aja.1000790302

All authors contributed to the article and approved the submitted version.

## Funding

This work was supported by the Department of Hebei Provincial Finance (2018034).

## Acknowledgments

The authors would like to thank Birong Li for polishing our paper and revising the pictures.

## Conflict of interest

The authors declare that the research was conducted in the absence of any commercial or financial relationships that could be construed as a potential conflict of interest.

## Publisher's note

All claims expressed in this article are solely those of the authors and do not necessarily represent those of their affiliated organizations, or those of the publisher, the editors and the reviewers. Any product that may be evaluated in this article, or claim that may be made by its manufacturer, is not guaranteed or endorsed by the publisher.

17. Cao C, Cerfolio RJ, Louie BE, Melfi F, Veronesi G, Razzak R, et al. Incidence, management, and outcomes of intraoperative catastrophes during robotic pulmonary resection. *Ann Thorac Surg* (2019) 108(5):1498–504. doi: 10.1016/j.athoracsur.2019.05.020
18. Wu W-B, Xu X-F, Wen W, Xu J, Zhu Q, Pan X-L, et al. Three-dimensional computed tomography bronchography and angiography in the preoperative evaluation of thoracoscopic segmentectomy and subsegmentectomy. *J Thorac Dis* (2016) 8:S710–S5. doi: 10.21037/jtd.2016.09.43
19. Tongxin L, Jing X, Runyuan W, Wei W, Yu Z, Dong W, et al. Application research of three-dimensional printing technology and three-dimensional computed tomography in segmentectomy. *Front Surg* (2022) 9:881076. doi: 10.3389/fsurg.2022.881076
20. Fukuhara K, Akashi A, Nakane S, Tomita E. Preoperative assessment of the pulmonary artery by three-dimensional computed tomography before video-assisted thoracic surgery lobectomy. *Eur J Cardiothorac Surg* (2008) 34(4):875–7. doi: 10.1016/j.ejcts.2008.07.014
21. Zhang M, Sun WJ, Wu QC, Ge MJ. Boyden's triad in the left lung: an interesting phenomenon. *Interact Cardiovasc Thorac Surg* (2022) 35(2). doi: 10.1093/icvts/ivac082
22. Yaginuma H. Investigation of displaced bronchi using multidetector computed tomography: associated abnormalities of lung lobulations, pulmonary arteries and veins. *Gen Thorac Cardiovasc Surg* (2020) 68(4):342–9. doi: 10.1007/s11748-019-01223-2
23. Hayashi K, Motoishi M, Horimoto K, Sawai S, Hanaoka J. Left upper division segmentectomy with a simultaneous displaced bronchus and pulmonary arteriovenous anomalies: a case report. *J Cardiothorac Surg* (2018) 13(1):40. doi: 10.1186/s13019-018-0741-6